The Potential of Unique Words in OFDM

Mario Huemer[1], Christian Hofbauer[1] and Johannes B. Huber[2]
[1]Klagenfurt University, Institute of Networked and Embedded Systems, A-9020 Klagenfurt
[2]University of Erlangen-Nuremberg, Institute for Information Transmission, D-91058 Erlangen
mario.huemer@uni-klu.ac.at, chris.hofbauer@uni-klu.ac.at, huber@lnt.de

***Abstract*— In this paper we propose a novel transmit signal structure and an adjusted and optimized receiver for OFDM (orthogonal frequency division multiplexing). Instead of the conventional cyclic prefix (CP) we use a deterministic sequence, which we call unique word (UW), as guard interval. We show how unique words, which are already well investigated for single carrier frequency domain equalization (SC/FDE) systems, can also be introduced in OFDM symbols. Since unique words represent known sequences, they can advantageously be used for synchronization and channel estimation purposes. Furthermore, the proposed approach introduces correlations along the subcarrier symbols. This allows to apply a highly efficient Wiener LMMSE (linear minimum mean square error) smoother for noise reduction at the receiver. We present simulation results in an indoor multipath environment to highlight the advantageous properties of the proposed scheme.**

I. Introduction

In conventional OFDM signaling, subsequent symbols are separated by guard intervals, which are usually implemented as cyclic prefixes [1]. In this paper, we propose to use known sequences, which we call unique words, instead of cyclic prefixes. The technique of using UWs has already been investigated in-depth for SC/FDE systems [2], where the introduction of unique words in time domain is straightforward, since the data symbols are also defined in time domain [3]. In this paper, we will show how unique words can also be introduced in OFDM time domain symbols, even though the data QAM (quadrature amplitude modulation) symbols are defined in frequency domain. Furthermore, we will introduce an optimized receiver concept adjusted to the novel transmit signal structure.

Fig. 1 compares the transmit data structure of CP- and UW-based transmission in time domain. Both structures make sure that the linear convolution of an OFDM symbol with the impulse response of a dispersive (e.g. multipath) channel appears as a cyclic convolution at the receiver side. Nevertheless, there are also some fundamental differences between CP- and UW-based transmission:

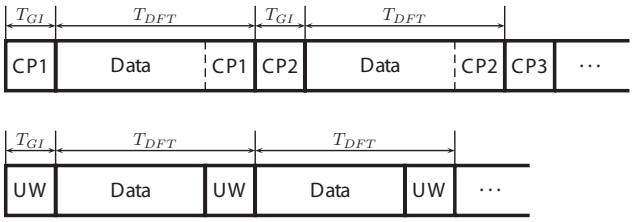

Fig. 1: Transmit data structure using CPs (above) or UWs (below).

- The UW is part of the DFT (discrete Fourier transform) interval, whereas the CP is not. Previous attempts of applying UWs to OFDM suffered from a substantial loss in bandwidth efficiency [4]. Although we need to spend dedicated subcarriers - which we call redundant subcarriers - for creating a UW in the time domain, we achieve approximately the same bandwidth efficiency in our approach as in conventional CP-OFDM. This is due to the fact that the length of one OFDM symbol reduces from $T_{DFT} + T_{GI}$ to T_{DFT}.
- The CP is random, whereas the UW is a known deterministic sequence. Therefore, the UW can advantageously be utilized for synchronization [5] and channel estimation purposes [6].

Both statements hold for OFDM- as well as for SC/FDE-systems. However, in OFDM - different to SC/FDE - the introduction of UWs in time domain leads to another fundamental and beneficial signal property: A UW in time domain generates a word of a complex number RS (Reed Solomon)-code along the subcarrier symbols [7]. Another interpretation of this fact which we prefer here, is an introduction of correlations along the subcarriers. These correlations can advantageously be used as a-priory knowledge at the receiver to significantly improve the BER (bit error ratio) performance by applying a simple LMMSE Wiener smoother succeeding the common zero forcing (ZF) equalizer.

Christian Hofbauer has been funded by the European Regional Development Fund and the Carinthian Economic Promotion Fund (KWF) under grant 20214/15935/23108.

The rest of the paper is organized as follows: In section II we describe our approach of how to introduce UWs in OFDM symbols. Section III introduces an LMMSE receiver that exploits the correlations introduced at the transmitter side. In section IV the novel UW-OFDM concept is compared to the classical CP-OFDM by means of simulation results. For this, the IEEE 802.11a WLAN (wireless local area networks) standard serves as reference system.

Notation

Lower-case bold face variables ($\mathbf{a}, \mathbf{b}$,...) indicate vectors, and upper-case bold face variables ($\mathbf{A}, \mathbf{B}$,...) indicate matrices. To distinguish between time and frequency domain variables, we use a tilde to express frequency domain vectors and matrices ($\tilde{\mathbf{a}}, \tilde{\mathbf{A}}$,...), respectively. We further use $\mathbb{C}$ to denote the set of complex numbers, $\mathbf{I}$ to denote the identity matrix, $(\cdot)^T$ to denote transposition, $(\cdot)^H$ to denote conjugate transposition, and $E[\cdot]$ to denote expectation.

II. Generation of UWs in OFDM Symbols

In conventional CP-OFDM, the data vector $\tilde{\mathbf{d}} \in \mathbb{C}^{N_d \times 1}$ is defined in the frequency domain. Typically, zero subcarriers are inserted at the band edges and at the DC subcarrier position, which can mathematically be described by a matrix operation $\tilde{\mathbf{x}} = \mathbf{B}\tilde{\mathbf{d}}$ with $\tilde{\mathbf{x}} \in \mathbb{C}^{N \times 1}$ and $\mathbf{B} \in \mathbb{C}^{N \times N_d}$. $\mathbf{B}$ consists of zero-rows at the positions of the zero subcarriers, and of appropriate unit row vectors at the positions of data subcarriers. The vector $\tilde{\mathbf{x}}$ denotes the OFDM symbol in frequency domain. The vector of time domain samples $\mathbf{x} \in \mathbb{C}^{N \times 1}$ is calculated via an IDFT (inverse DFT) operation $\mathbf{x} = \mathbf{F}_N^{-1}\tilde{\mathbf{x}}$, where $\mathbf{F}_N$ denotes the N-point DFT matrix.

We now modify this conventional approach by introducing a pre-defined sequence $\mathbf{x}_u \in \mathbb{C}^{N_u \times 1}$, which we call unique word, and which shall form the tail of the time domain vector, which we now denote by $\mathbf{x}'$. Hence, $\mathbf{x}'$ is given by $\mathbf{x}' = \begin{bmatrix}\mathbf{x}_d^T & \mathbf{x}_u^T\end{bmatrix}^T$, whereas only $\mathbf{x}_d \in \mathbb{C}^{(N-N_u) \times 1}$ is random and affected by the data. We use a two-step approach for the generation of the so-defined vector $\mathbf{x}'$:

- Generate a zero UW such that $\mathbf{x} = \begin{bmatrix}\mathbf{x}_d^T & \mathbf{0}^T\end{bmatrix}^T$ and $\mathbf{x} = \mathbf{F}_N^{-1}\tilde{\mathbf{x}}$.
- Add the UW in time domain such that $\mathbf{x}' = \mathbf{x} + \begin{bmatrix}\mathbf{0}^T & \mathbf{x}_u^T\end{bmatrix}^T$.

We now describe the first step in detail: As in conventional OFDM, the QAM data symbols and the zero subcarriers are specified in frequency domain in vector $\tilde{\mathbf{x}}$, but here in addition the zero-word is specified in time domain as part of the vector $\mathbf{x}$. As a consequence, the linear system of equations $\mathbf{x} = \mathbf{F}_N^{-1}\tilde{\mathbf{x}}$ can only be fulfilled by reducing the number N_d of data subcarriers, and by introducing a set of redundant subcarriers instead. We let the redundant subcarriers form the vector $\tilde{\mathbf{r}} \in \mathbb{C}^{N_r \times 1}$ with $N_r = N_u$, further introduce a permutation matrix $\mathbf{P} \in \mathbb{C}^{(N_d+N_r)\times(N_d+N_r)}$, and form an OFDM symbol (containing $N - N_d - N_r$ zero subcarriers) in frequency domain by

$$\tilde{\mathbf{x}} = \mathbf{B}\mathbf{P}\begin{bmatrix}\tilde{\mathbf{d}} \\ \tilde{\mathbf{r}}\end{bmatrix}. \tag{1}$$

We will detail the reason for the introduction of the permutation matrix and its specific construction shortly below. $\mathbf{B} \in \mathbb{C}^{N \times (N_d+N_r)}$ is again a trivial matrix that inserts the usual zero subcarriers. Fig. 2 illustrates this approach in a graphical way.

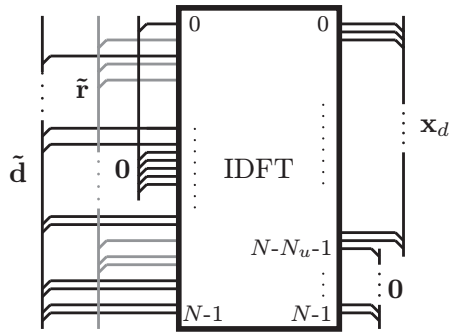

Fig. 2: Time- and frequency-domain view of an OFDM symbol in UW-OFDM.

The time - frequency relation of the OFDM symbol can now be written as

$$\mathbf{F}_N^{-1}\mathbf{B}\mathbf{P}\begin{bmatrix}\tilde{\mathbf{d}} \\ \tilde{\mathbf{r}}\end{bmatrix} = \begin{bmatrix}\mathbf{x}_d \\ \mathbf{0}\end{bmatrix}. \tag{2}$$

With $\mathbf{M} = \mathbf{F}_N^{-1}\mathbf{B}\mathbf{P} = \begin{bmatrix}\mathbf{M}_{11} & \mathbf{M}_{12} \\ \mathbf{M}_{21} & \mathbf{M}_{22}\end{bmatrix}$, where $\mathbf{M}_{ij}$ are appropriate sized sub-matrices, it follows that $\mathbf{M}_{21}\tilde{\mathbf{d}} + \mathbf{M}_{22}\tilde{\mathbf{r}} = \mathbf{0}$, and hence $\tilde{\mathbf{r}} = -\mathbf{M}_{22}^{-1}\mathbf{M}_{21}\tilde{\mathbf{d}}$. With the matrix $\mathbf{T} = -\mathbf{M}_{22}^{-1}\mathbf{M}_{21}$ ($\mathbf{T} \in \mathbb{C}^{N_r \times N_d}$), the vector of redundant subcarrier symbols can thus be determined by the linear mapping

$$\tilde{\mathbf{r}} = \mathbf{T}\tilde{\mathbf{d}}. \tag{3}$$

In the style of block coding theory, we use the notation

$$\tilde{\mathbf{c}} = \mathbf{P}\begin{bmatrix}\tilde{\mathbf{d}} \\ \tilde{\mathbf{r}}\end{bmatrix} = \mathbf{P}\begin{bmatrix}\mathbf{I} \\ \mathbf{T}\end{bmatrix}\tilde{\mathbf{d}} = \mathbf{G}\tilde{\mathbf{d}} \tag{4}$$

($\tilde{\mathbf{c}} \in \mathbb{C}^{(N_d+N_r)\times 1}$, $\mathbf{G} \in \mathbb{C}^{(N_d+N_r)\times N_d}$) for the non-zero part of $\tilde{\mathbf{x}}$, such that $\tilde{\mathbf{x}} = \mathbf{B}\tilde{\mathbf{c}}$. $\mathbf{G}$ can be interpreted as a code generator matrix, and $\tilde{\mathbf{c}}$

corresponds to a word of a complex number RS-code. Another interpretation is that $\mathbf{G}$ introduces correlations in the vector $\tilde{\mathbf{x}}$ of frequency domain samples of an OFDM symbol.

In the second step, the transmit symbol $\mathbf{x}'$ is generated by adding the unique word: $\mathbf{x}' = \mathbf{x} + \begin{bmatrix}\mathbf{0}^T & \mathbf{x}_u^T\end{bmatrix}^T$. The frequency domain version $\tilde{\mathbf{x}}_u \in \mathbb{C}^{N\times 1}$ of the UW is defined by $\tilde{\mathbf{x}}_u = \mathbf{F}_N \begin{bmatrix}\mathbf{0}^T & \mathbf{x}_u^T\end{bmatrix}^T$. Note that $\mathbf{x}'$ can also be written as $\mathbf{x}' = \mathbf{F}_N^{-1}(\tilde{\mathbf{x}} + \tilde{\mathbf{x}}_u) = \mathbf{F}_N^{-1}(\mathbf{B}\tilde{\mathbf{c}} + \tilde{\mathbf{x}}_u)$.

A very critical aspect of UW-OFDM is the optimum distribution of the redundant subcarriers over the available bandwidth [7]. A suboptimum placement may lead to extremely high energy contributions of the redundant subcarriers to the mean energy $E_{\mathbf{x}'} = E[(\mathbf{x}')^H\mathbf{x}']$ of the transmit symbol $\mathbf{x}'$. $E_{\mathbf{x}'}$ can easily shown to be

$$E_{\mathbf{x}'} = \frac{1}{N}(\underbrace{N_d\sigma_d^2}_{E_{\tilde{\mathbf{d}}}} + \underbrace{\sigma_d^2\mathrm{tr}(\mathbf{T}\mathbf{T}^H)}_{E_{\tilde{\mathbf{r}}}}) + \underbrace{\mathbf{x}_u^H\mathbf{x}_u}_{E_{\mathbf{x}_u}}. \quad (5)$$

It turns out that the energy contribution $\frac{E_{\tilde{\mathbf{r}}}}{N}$ of the redundant subcarrier symbols almost explodes without the use of the permutation matrix. The problem can be solved by an optimized permutation of the data and redundant subcarrier symbols. We thus select $\mathbf{P}$ such that $\mathrm{tr}\left(\mathbf{T}\mathbf{T}^H\right)$ becomes minimum, which provides minimum energy on the redundant subcarriers on average (when averaging over all possible data vectors $\tilde{\mathbf{d}}$).

III. LMMSE UW-OFDM Receiver

After the transmission over a multipath channel and after the common DFT operation (preferably implemented as FFT (fast Fourier transform)), the non-zero part $\tilde{\mathbf{y}} \in \mathbb{C}^{(N_d+N_r)\times 1}$ of a received OFDM frequency domain symbol can be modeled as

$$\tilde{\mathbf{y}} = \mathbf{B}^T\mathbf{F}_N\mathbf{H}\mathbf{F}_N^{-1}(\mathbf{B}\tilde{\mathbf{c}} + \tilde{\mathbf{x}}_u) + \mathbf{B}^T\mathbf{F}_N\mathbf{n}, \quad (6)$$

where $\mathbf{H}$ denotes a cyclic convolution matrix with $\mathbf{H} \in \mathbb{C}^{N\times N}$, and $\mathbf{n} \in \mathbb{C}^{N\times 1}$ represents a noise vector with the covariance matrix $\sigma_n^2\mathbf{I}$. The multiplication with $\mathbf{B}^T$ excludes the zero subcarriers from further operation. The matrix $\mathbf{F}_N\mathbf{H}\mathbf{F}_N^{-1}$ is diagonal and contains the sampled channel frequency response on its main diagonal. $\tilde{\mathbf{H}} = \mathbf{B}^T\mathbf{F}_N\mathbf{H}\mathbf{F}_N^{-1}\mathbf{B}$ with $\tilde{\mathbf{H}} \in \mathbb{C}^{(N_d+N_r)\times(N_d+N_r)}$ is a down-sized version of the latter excluding the entries corresponding to the zero subcarriers. The received symbol can thus be written as

$$\tilde{\mathbf{y}} = \tilde{\mathbf{H}}\tilde{\mathbf{c}} + \tilde{\mathbf{H}}\mathbf{B}^T\tilde{\mathbf{x}}_u + \tilde{\mathbf{v}} \quad (7)$$

with the noise vector $\tilde{\mathbf{v}} = \mathbf{B}^T\mathbf{F}_N\mathbf{n}$. Note that (assuming that the channel matrix $\tilde{\mathbf{H}}$ or at least an estimate of the same is available) $\tilde{\mathbf{H}}\mathbf{B}^T\tilde{\mathbf{x}}_u$ represents a known signal contained in the received symbol $\tilde{\mathbf{y}}$. In order to determine the Bayesian LMMSE estimator, let $\tilde{\mathbf{y}}' = \tilde{\mathbf{y}} - \tilde{\mathbf{H}}\mathbf{B}^T\tilde{\mathbf{x}}_u$ such that $\tilde{\mathbf{y}}' = \tilde{\mathbf{H}}\tilde{\mathbf{c}} + \tilde{\mathbf{v}}$. By applying the Bayesian Gauss-Markov theorem [8], the LMMSE estimator follows to

$$\widehat{\tilde{\mathbf{c}}} = \mathbf{C}_{\tilde{c}\tilde{c}}\tilde{\mathbf{H}}^H(\tilde{\mathbf{H}}\mathbf{C}_{\tilde{c}\tilde{c}}\tilde{\mathbf{H}}^H + \mathbf{C}_{\tilde{v}\tilde{v}})^{-1}\tilde{\mathbf{y}}'. \quad (8)$$

With the noise covariance matrix $\mathbf{C}_{\tilde{v}\tilde{v}} = E\left[\tilde{\mathbf{v}}\tilde{\mathbf{v}}^H\right] = N\sigma_n^2\mathbf{I}$, and with $\mathbf{C}_{\tilde{c}\tilde{c}} = E\left[\tilde{\mathbf{c}}\tilde{\mathbf{c}}^H\right] = \sigma_d^2\mathbf{G}\mathbf{G}^H$ (here we assumed uncorrelated and zero-mean data QAM symbols with variance σ_d^2), (8) can immediately be re-written as

$$\widehat{\tilde{\mathbf{c}}} = \tilde{\mathbf{W}}\tilde{\mathbf{H}}^{-1}(\tilde{\mathbf{y}} - \tilde{\mathbf{H}}\mathbf{B}^T\tilde{\mathbf{x}}_u) \quad (9)$$

with the Wiener smoothing matrix defined as

$$\tilde{\mathbf{W}} = \mathbf{G}\mathbf{G}^H\left(\mathbf{G}\mathbf{G}^H + \frac{N\sigma_n^2}{\sigma_d^2}(\tilde{\mathbf{H}}^H\tilde{\mathbf{H}})^{-1}\right)^{-1}. \quad (10)$$

Finally, the data part $\widehat{\tilde{\mathbf{d}}} = \begin{bmatrix}\mathbf{I} & \mathbf{0}\end{bmatrix}\mathbf{P}^{-1}\widehat{\tilde{\mathbf{c}}}$ can be processed further as usual.

We summarize the receiver operations per OFDM symbol:

- Perform an FFT operation and remove the zero subcarriers to obtain $\tilde{\mathbf{y}}$.
- Eliminate the influence of the UW by subtracting $\tilde{\mathbf{H}}\mathbf{B}^T\tilde{\mathbf{x}}_u$ from $\tilde{\mathbf{y}}$.
- Apply ZF equalization ($\tilde{\mathbf{H}}^{-1}$) followed by
- the Wiener smoothing operation ($\tilde{\mathbf{W}}$).
- Extract the data part and process further as usual.

Of course, the zero forcing and the smoothing operation can be implemented in one combined single matrix multiplication operation. Furthermore we mention, that the influence of the UW could also by eliminated after ZF by simply subtracting $\mathbf{B}^T\tilde{\mathbf{x}}_u$.

We notice that the error $\tilde{\mathbf{e}} = \tilde{\mathbf{c}} - \widehat{\tilde{\mathbf{c}}}$ has zero mean, and its covariance matrix is given by $\mathbf{C}_{\tilde{e}\tilde{e}} = \left(\mathbf{I} - \tilde{\mathbf{W}}\right)\mathbf{C}_{\tilde{c}\tilde{c}}$ [8]. In our system simulations, the main diagonal elements of matrix $\mathbf{C}_{\tilde{e}\tilde{e}}$ corresponding to data entries are used in a soft decision Viterbi decoder to specify the varying noise variances along the data symbols after ZF equalization and Wiener smoothing.

IV. Simulation Results

Fig. 3 shows the block diagram of the simulated UW-OFDM system (equivalent complex baseband

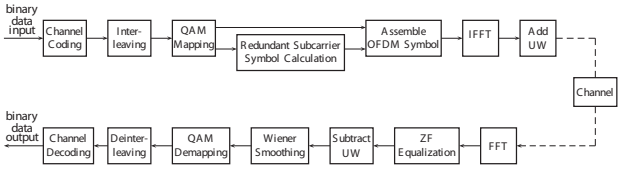

Fig. 3: Block diagram for simulation analysis.

description is used throughout this paper). After channel coding, interleaving and QAM-mapping, the redundant subcarrier symbols are determined using (3). After assembling the OFDM symbol, which is composed of $\tilde{\mathbf{d}}$, $\tilde{\mathbf{r}}$, and a set of zero subcarriers, the IFFT (inverse FFT) is performed. Finally, the UW is added in the time domain. At the receiver the FFT operation is followed by a ZF equalization as in classical CP-OFDM. Next, the frequency domain version of the UW is subtracted. Then the Wiener smoother is applied to the symbol, and finally demapping, deinterleaving and decoding is performed. For the soft decision Viterbi decoder matrix $\mathbf{C}_{\tilde{e}\tilde{e}}$ is exploited as described above.

We compare our novel UW-OFDM approach with the classical CP-OFDM concept. The IEEE 802.11a WLAN standard [9] serves as reference system.

TABLE I: MAIN PHY PARAMETERS OF 802.11A AND THE INVESTIGATED UW-OFDM SYSTEM.

	802.11a	UW-OFDM
Modulation schemes	BPSK, QPSK, 16QAM, 64QAM	BPSK, QPSK, 16QAM, 64QAM
Coding rates	1/2, 2/3, 3/4	1/2, 2/3, 3/4
FFT size	64	64
Data subcarriers	48	36
Additional subcarriers	4 (pilots)	16 (redundant)
DFT period	3.2 μs	3.2 μs
Guard duration	800 ns (CP)	800 ns (UW)
Total symbol duration	4 μs	3.2 μs

We apply the same parameters for UW-OFDM as in [9] wherever possible, the most important parameters are specified in table I. The zero subcarriers are chosen as in [9], the indices of the redundant subcarriers are chosen to be {2, 6, 10, 14, 17, 21, 24, 26, 38, 40, 43, 47, 50, 54, 58, 62}. This choice, which can easily also be described by (1) with an appropriately constructed matrix $\mathbf{P}$, minimizes the cost function $\mathrm{tr}\left(\mathbf{T}\mathbf{T}^H\right)$ discussed above.

In our approach the unique word shall take over the synchronization tasks which are normally performed with the help of the 4 pilot subcarriers. In order to make a fair comparison, the energy of the UW related to the total energy of a transmit symbol is set to 4/52, which exactly corresponds to the total energy of the 4 pilots related to the total energy of a transmit symbol in the IEEE standard. Note that the particular design of the UW has no impact on the BER behavior. In conventional CP-OFDM like in the WLAN standard, the total length of an OFDM symbol is given by $T_{GI} + T_{DFT}$. However, the guard interval is part of the DFT period in our approach. Therefore, both systems show comparable bandwidth efficiency.

The multipath channel has been modeled as a tapped delay line, each tap with uniformly distributed phase and Rayleigh distributed magnitude, and with power decaying exponentially. A detailed description of the model can be found in [6]. Fig. 4 shows two typical channel snapshots featuring an rms delay spread of 100ns. The frequency response of channel A features two spectral notches within the system's bandwidth, whereas channel B shows no deep fading holes.

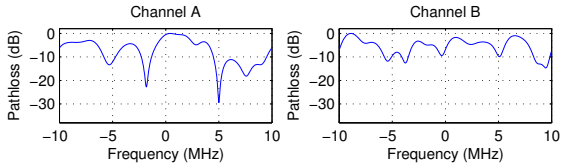

Fig. 4: Frequency-domain representation of two multipath channel snapshots (channel A, channel B).

Fig. 5 compares the mean squared errors on the $N_d + N_r$ (data + redundant) subcarriers before and after the Wiener smoothing operation when transmitting over channel A. We note that all subcarriers experience a significant noise reduction by the smoother, but the effect is impressive on the subcarriers corresponding to spectral notches in the channel frequency response. The subcarriers with indices 15 and 46 correspond to the spectral notches around 5MHz and -2MHz, respectively, cf. Fig. 4.

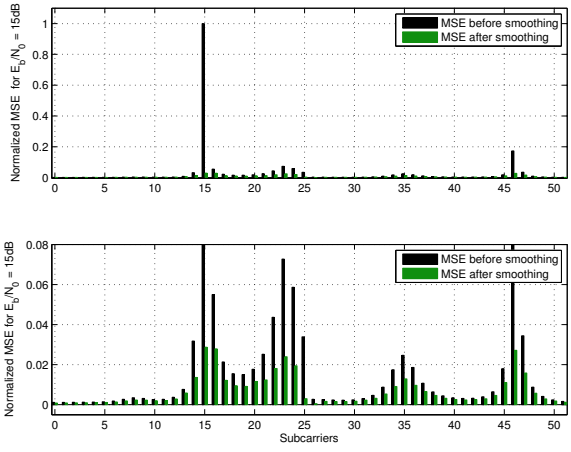

Fig. 5: Noise reduction effect of the Wiener smoother in a frequency selective environment (channel A) for E_b/N_0 = 15dB. Above: full scale; below: zoomed y-axis.

In Fig. 6 the BER-behavior of the IEEE 802.11a standard and the novel UW-OFDM approach are compared, both in QPSK-mode for the channel A (cf. Fig. 4). Here we show results of simulations with and without the usage of an additional outer code. The outer code features the coding rates $r = 3/4$ and $r = 1/2$, respectively. Both systems use the same convolutional coder with the industry standard rate 1/2, constraint length 7 code with generator polynomials (133,171). For $r = 3/4$ puncturing is used as described in [9]. Note that due to the different number of data symbols per OFDM symbol, the interleaver had to be slightly adapted compared to the WLAN standard. Perfect channel knowlegde is assumed in both approaches. In the case of no further outer code, i.e. $r = 1$, the gain achieved by the LMMSE smoother is impressive. This can be explained by the significant noise reduction on heavily attenuated subcarriers. For the coding rates $r = 3/4$ and $r = 1/2$, the novel UW-OFDM approach still achieves a gain of 0.9dB and 0.6dB at a bit error ratio of 10^{-6}, respectively. Fig. 7 shows the results for channel B, cf. Fig. 4. Even though the gains are reduced, we notice similar tendencies. We gain 0.9dB in case of $r = 1$, 0.7dB for $r = 3/4$ and 0.3dB for $r = 1/2$ (again at a BER of 10^{-6}).

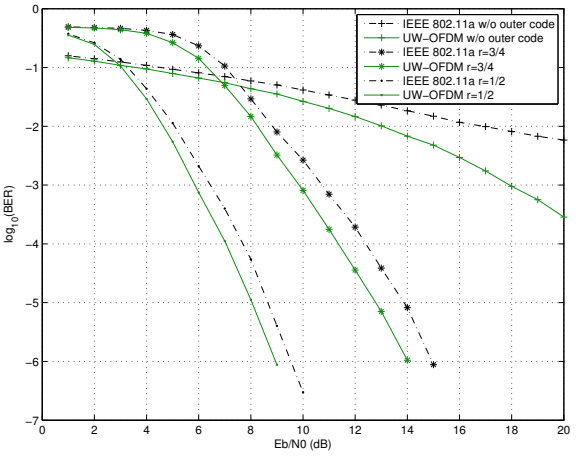

Fig. 6: Channel A - BER comparison between the novel UW-OFDM approach and the IEEE 802.11a OFDM based standard.

V. Conclusion

In this work we introduced a novel OFDM signaling concept, where the guard intervals are built by unique words instead of cyclic prefixes. The proposed approach introduces a complex number Reed-Solomon code structure within the sequence of subcarriers. As an important conclusion we can state, that besides the possibility to use the UW for synchronization and channel estimation purposes, the novel approach additionally allows to apply a highly efficient LMMSE Wiener smoother, which significantly reduces the noise on the subcarriers, especially on highly attenuated subcarriers. Simulation results illustrate that the novel approach outperforms classical CP-OFDM in typical frequency selective indoor scenarios.

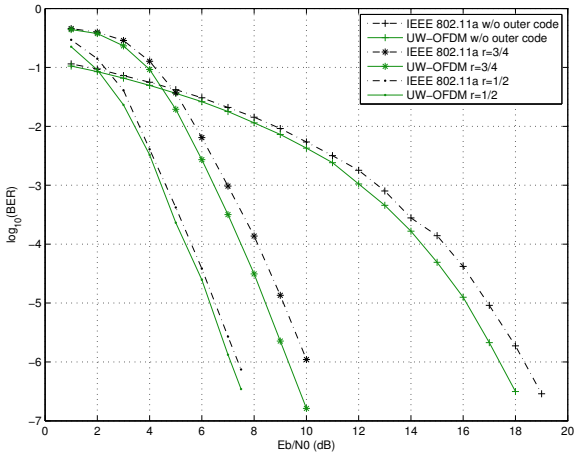

Fig. 7: Channel B - BER comparison between the novel UW-OFDM approach and the IEEE 802.11a OFDM based standard.

References

[1] R. van Nee, R. Prasad, *OFDM for Wireless Multimedia Communications*, Artech House Publishers, Boston, 2000.

[2] H. Sari, G. Karam, I. Jeanclaude, "Frequency-Domain Equalization of Mobile Radio and Terrestrial Broadcast Channels", In *Proceedings of the IEEE International Conference on Global Communications (GLOBECOM '94)*, San Francisco, USA, pages 1-5, 1994.

[3] L. Deneire, B. Gyselinckx, M. Engels, "Training Sequence vs. Cyclic Prefix: A New Look on Single Carrier Communication", In *Proceedings of the IEEE International Conference on Global Communications (GLOBECOM '2000)*, pages 1056-1060, November 2000.

[4] L. Jingyi, P. Joo, J. Ro, "The effect of filling Unique Words to guard interval for OFDM", Document IEEE C802.16a-02/87, IEEE 802.16 Broadband Wireless Access Working Group, September 2002.

[5] M. Huemer, H. Witschnig, J. Hausner, "Unique Word Based Phase Tracking Algorithms for SC/FDE Systems", In the *Proceedings of the IEEE International Conference on Global Communications (GLOBECOM' 2003)*, San Francisco, USA, 5 pages, December 2003.

[6] H. Witschnig, Frequency Domain Equalization for Broadband Wireless Communication - With Special Reference to Single Carrier Transmission Based on Known Pilot Sequences, Dissertation, University of Linz, Institute for Communications and Information Engineering, 2004.

[7] W. Henkel, F. Hu, I. Kodrasi, "Inherent Time-Frequency Coding in OFDM and ISI Correction without a Cyclic Prefix", In *Proceedings 14th International OFDM Workshop 2009*, Hamburg, Germany, September 2009.

[8] S. Kay, *Fundamentals of Statistical Signal Processing: Estimation Theory*, Prentice Hall, Rhode Island 1993.

[9] IEEE Std 802.11a-1999, Part 11: Wireless LAN Medium Access Control (MAC) and Physical Layer (PHY) specifications: High-Speed Physical Layer in the 5 GHz Band, 1999.